THE ASTROPHYSICAL JOURNAL, 463:L67–L70, 1996 June 1

REAL-TIME DETECTION AND MULTISITE OBSERVATIONS OF GRAVITATIONAL MICROLENSING

C. ALCOCK,[1,2] R. A. ALLSMAN,[3] D. ALVES,[1,4] T. S. AXELROD,[5] A. C. BECKER,[6] D. P. BENNETT,[1,2,7] K. H. COOK,[1,2,7] K. C. FREEMAN,[5] K. GRIEST,[2,8] J. GUERN,[2,8] M. J. LEHNER,[2,8] S. L. MARSHALL,[1,2,7] B. A. PETERSON,[5] M. R. PRATT,[2,6,7,9] P. J. QUINN,[5] D. REISS,[6] A. W. RODGERS,[5] C. W. STUBBS,[2,5,6,7,9] W. SUTHERLAND,[10] AND D. L. WELCH[11] (THE MACHO COLLABORATION)

Received 1996 January 23; accepted 1996 March 7

ABSTRACT

The MACHO collaboration is carrying out an extensive survey to detect gravitational microlensing. We have recently demonstrated the ability to detect candidate microlensing events in real time, often well before the peak amplification of the event. This has made possible the acquisition of spectra over the course of an event, the invariance of which has lent strong support to the microlensing interpretation. This paper reports on photometric data that were acquired from two sites, Cerro Tololo Inter-American Observatory and Mount Stromlo, in response to the real time detection of a microlensing event. The superior photometry obtained from Chile and the complementary time coverage demonstrate the viability of mounting an aggressive campaign of microlensing follow-up observations.

Subject headings: dark matter — gravitational lensing — stars: low-mass, brown dwarfs

1. INTRODUCTION

Three groups have now published detections of candidate microlensing events. Our MACHO collaboration has reported on the analysis of our first year's data, in which we detected three candidate events toward the Large Magellanic Cloud (LMC) (Alcock et al. 1993, 1995a, 1996a) and ~45 events toward the Galactic bulge (Bennett et al. 1994; Alcock et al. 1995b, 1996b). The EROS collaboration has reported two events toward the LMC (Aubourg et al. 1993; Ansari et al. 1995), and the OGLE collaboration has reported a total of 12 events toward the Galactic bulge (Udalski et al. 1993, 1994a). Also, three further groups have observations in progress; the DUO collaboration has ~12 preliminary candidates toward the bulge, and the AGAPE and VATT-Columbia groups have begun searches for microlensing toward M31.

The microlensing rate along lines of sight toward the LMC will constrain the contribution of MACHOs to the mass of the Galaxy (Paczyński 1986; Griest 1991). In addition, microlensing observations toward the Galactic center are playing an important role in improving our understanding of Galactic structure (Griest et al. 1991; Paczyński 1991). Taken in conjunction with rotation curve data, diffuse IR light (Weiland et al. 1994; Dwek et al. 1995), and star counts, the Galactic center microlensing observations set important constraints on models of the mass distribution of the Galaxy and thereby also have a direct impact on the dark matter problem. Our microlensing search is structured to obtain as many microlensing events as possible. To achieve this, the photometric accuracy and time sampling are limited not only by the seeing and weather at the Mount Stromlo site but also by the compromise between the number of fields monitored and the frequency of observations for each field. However, some of the most exciting and important possible discoveries in microlensing require both higher accuracy and finer sampling. In 1994 June, we acquired the ability to detect microlensing events in real time, allowing for supplemental observing campaigns during the course of an event.

Real-time detection of microlensing (1) makes possible spectroscopy of the lensed star *during* the event, both to ascertain spectral invariance and to exploit the lensing process to investigate faint stars; (2) allows for coordinated observations from multiple sites to overcome weather problems and to increase coverage in the time domain; (3) makes high-accuracy photometry of an event possible without sacrificing the overall event detection rate of the survey system; (4) provides increased discrimination between genuine lensing events and background processes; and, in particular, (5) increases the likelihood of detecting light-curve fine structure.

The canonical model of a microlensing event assumes a point source, a point lens, and constant relative speed between the source-observer line of sight and the lens. The resulting light curve is then achromatic and symmetric with the standard shape determined by three parameters: $A_{\max}$, the maximum amplification; t_0, the time of maximum amplification; and $\hat{t}$, the event timescale. Of the three parameters, only the timescale provides information about the lens. Finer, more accurate sampling of ongoing events may allow the detection and characterization of events that deviate from the canonical light-curve shape. Such events can be caused by genuine microlensing involving binary sources, binary lenses, lenses with planets, sources with finite angular dimension, and parallax effects caused by the noninertial relative motion between the source-observer line of sight and the lens. All of these effects involve extra parameters in a fit to the light-curve

[1] Lawrence Livermore National Laboratory, Livermore, CA 94550.
[2] Center for Particle Astrophysics, University of California, Berkeley, Berkeley, CA 94720.
[3] Supercomputing Facility, Australian National University, Canberra, ACT 0200, Australia.
[4] Department of Physics, University of California, Davis, Davis, CA 95616.
[5] Mount Stromlo and Siding Spring Observatories, Australian National University, Weston, ACT 2611, Australia.
[6] Departments of Astronomy and Physics, University of Washington, Seattle, WA 98195.
[7] Visiting Astronomer, Cerro Tololo Inter-American Observatory, National Optical Astronomy Observatory, operated by the Association of Universities for Research in Astronomy, Inc. (AURA) under cooperative agreement with the National Science Foundation.
[8] Department of Physics, University of California, San Diego, San Diego, CA 92039.
[9] Department of Physics, University of California, Santa Barbara, Santa Barbara, CA 93106.
[10] Department of Physics, University of Oxford, Oxford OX1 3RH, U.K.
[11] McMaster University, Hamilton, Ontario Canada L8S 4M1.

shape, and to constrain them will usually require more points and smaller errors.

For source stars the angular radii of which are comparable to the impact parameter, the transit of the lens across the source star generates deviations from the point-source light curve (Gould 1994; Witt & Mao 1994). If such deviations are measured, then the angular radius of the star may be estimated from its spectral type, giving a measurement of the proper angular motion of the lens.

Binary lensing is expected in perhaps 5%–10% of bulge microlensing events, and three binary lens events have been reported so far (Udalski et al. 1994c; Pratt et al. 1995; Alard, Mao, & Guibert 1995). When a binary lens system has a separation comparable to the Einstein radius, the two lenses conspire to produce light curves with a complex morphology. In particular, caustic crossings produce sharp spikes the width of which can be used to constrain the size of the source star (Bennett et al. 1995). Considerably more exciting is the possibility to observe microlensing by stars with a planet (Mao & Paczyński 1991; Gould & Loeb 1992) as the second component in the binary lens signature.

Finally, the higher quality light curves provide a check of the main survey program. There may well be events that trigger the real-time detection system and subsequently fail to pass the cuts in the main program because of poor coverage, large errors, or noncanonical shape. Also, for events that are detected by the main program, the independent photometry from the additional site(s) can verify that the events are not due to systematic error in the Mount Stromlo data.

The gravitational microlensing event reported here was the first ongoing event detected by our collaboration and was also the first microlensing event ever announced before peak amplification (Alcock et al. 1994). (The OGLE team has also detected ongoing microlensing events [Udalski et al. 1994b]). A variety of observations were undertaken during the course of this event. High-quality spectra were obtained by Benetti and colleagues (Benetti, Pasquini, & West 1995) from ESO. The observed spectral invariance lends strong support to the microlensing interpretation. The OGLE group also published photometry acquired during the event (Szymanski et al. 1994).

2. REAL-TIME DETECTION OF MICROLENSING

The MACHO project uses a dedicated telescope and wide-field camera system at Mount Stromlo to monitor fields in the Magellanic Clouds and Galactic bulge on a nightly basis, seeking the rare transient brightening that is the signature of gravitational microlensing. This experiment has been described in some detail elsewhere (Stubbs et al. 1993; Marshall et al. 1994; Alcock et al. 1995b).

An image of each field that was obtained in good seeing under dark skies is used as a "template" frame for subsequent photometry of that field: the stellar centroids and fluxes from the template frame are used to warm-start the photometry of other observations. Photometry is performed on the ~80 fields acquired per night with a version of DoPhot (Schecter, Mateo, & Saha 1993) modified to use prior knowledge of stellar centers. Fiducial stars are used to construct point-spread function (PSF) parameters and to normalize the measured fluxes in each frame, essentially bringing them into conformity with the zero point of the template frame. If a star shows a change in flux (in either passband) by 10% or more from its template value, it is flagged. If the ratio of the deviation to the estimated photometric error is larger than 7.0, the excursion is logged in an "alert" file. A set of criteria is applied to each data point, involving the χ^2 of the PSF fit, crowding, cosmic-ray information, etc., and unreliable data points are rejected. This star list is compared with a catalog of variable stars (generated in the full analysis of our data), and the known variables are excluded at this point. Any remaining exceptions are fitted to see if they lie along a line in the focal plane, which is an effective technique for rejecting satellite tracks and anomalies from aircraft lights. After excluding alert stars that lie along any fitted satellite tracks, any frame with over 10 alert stars is assumed to be an anomalous frame, and all triggers from the frame are rejected. These are usually due to poor telescope tracking; approximately 3% of alert frames are rejected by this criterion. On the other hand, if 10 or fewer triggers are detected in a frame, then they are reported by the alert system. (At the present time, any "new" stars that have no counterpart in the template frame go into the "alert" file but are not added to the template catalog, and hence they are not analyzed.) This procedure is executed for all observations of MACHO fields for which at least 1 yr of light-curve data is available. The remaining stars with unaccounted flux increases are then designated as interesting "alert" objects, and their dual-color photometric time series is automatically extracted from the database of MACHO photometry and distributed across the collaboration. This entire process requires no human intervention. There are typically about eight to 10 stars per night that emerge from the alert analysis. Their light curves are inspected by eye at this stage. Most of the alert light curves show anomalous single-point excursions (of either sign). A small fraction are uncataloged variable stars that are added to the variable star catalog to prevent further alerts. In a few cases, there is evidence of an upturn in the data over several consecutive observations that might reflect the start of a lensing event. In these cases, an alert notification is sent out by e-mail and posted on the World Wide Web.

Our team has reported over 40 candidate microlensing events in real time. We maintain a World Wide Web page, http://darkstar.astro.washington.edu, that summarizes the status of MACHO alert events. Individuals or organizations that wish to receive e-mail notification of newly detected events should request this by sending a message to macho@astro.washington.edu.

3. JOINT PHOTOMETRY RESULTS

On 1994 August 30 one of the stars we monitor in the Galactic bulge was observed to have a significant brightening over several nights. Designated alert 94-1, the star is at $\alpha = 17^h59^m49\overset{s}{.}6$ and $\delta = -28°10'56''$ (J2000). The source star has unamplified magnitudes of $R \sim 18.0$ and $V \sim 19.0$ and was constant in our 1993 data set. The images from the MACHO system at Mount Stromlo were processed with our standard photometry pipeline.

3.1. *Cerro Tololo Inter-American Observatory (CTIO) Images*

Our team has obtained a portion of each night on the 0.9 m telescope at CTIO, which we have used to follow microlensing events and to perform photometric calibrations. The CTIO observations are typically acquired during a single interval of 60–90 minutes each night. The list of target objects, along with desired exposure times and filters, are downloaded to a dedicated computer in the 0.9 m dome at CTIO. We read out

a 1024×1024 central subsection of the thinned Tektronix 2048^2 CCD detector, giving a field size of 7.′5 by 7.′5.

One hundred four 600 s R-band images of the alert field were taken during the period 1994 September 1 to October 4. Each image was bias subtracted and flat-field corrected using calibration images that were updated about once per week. The alert star was located by eye in each frame, and a 256×256 pixel subregion centered on the alert star was cut out to include in the photometric analysis.

To carry out the photometric reductions, a set of scripts written in PERL were developed that automate the DAOPHOT/ALLSTAR (Stetson 1987) sequence. First, a PSF was derived for each frame. A best frame was chosen to use as a "template" for all the reductions. A template reduction was carried out on the best seeing frame (taken on September 7) that yielded 3557 stars in the $\sim 1.'9 \times 1.'9$ frame. The PSF star lists were used to derive approximate coordinate and magnitude transformations between template image and the remaining "regular" frames. For each regular image, an input coordinate file for ALLSTAR was constructed by translating the coordinates and magnitudes in the template photometry file. A single ALLSTAR run (with floating positions) was then carried out on each image. Five of the frames failed at the coordinate transformation stage, leaving 99 images for the time series. The median number of stars converging was 2954, with as few as 636 in some frames with poor seeing or focus.

The photometric time series were made using the program DAOMASTER (Stetson 1992) with a final adjustment to a set of fiducial stars. Time series were generated for 1940 stars. Stars appearing in less than 40 of the 99 frames were not included. A set of 40 small-error, low-dispersion stars was chosen as final fiducial relative magnitude calibrators. Magnitude offsets needed to maintain the average magnitude of the fiducial set were calculated and applied to generate a final set of ASCII time series files. Also, the reported magnitude errors (DAOPHOT) for the alert star were increased by a factor of 1.7 to account for the typical scatter in the time series of constant stars from this same data set.

4. DISCUSSION

The CTIO and Mount Stromlo photometric data were subjected to a joint fit to a theoretical microlensing light curve that assumes a point source and a point lens. The flux f_i in each of the three passbands, ($i = r, b, R$), was fitted to an independent baseline, f_{0i}, and a single amplification function, $A(t; t_0, \hat{t}, u_{\min})$, that depends upon the time of peak amplification, t_0, the minimum impact parameter in units of the system's Einstein ring radius, $u_{\min}$, and the time, $\hat{t}$, for the lens to move by two Einstein ring radii relative to the undeflected observer-source line of sight. The three data sets were fitted to a triplet of equations of the form

$$f_i(t) = f_{0i}\, A(t), \quad i = r, b, R, \tag{1}$$

with

$$A = \frac{u^2 + 2}{u\sqrt{u^2 + 2}}; \quad u(t) \equiv \sqrt{u_{\min}^2 + \left[\frac{2(t - t_0)}{\hat{t}}\right]^2}. \tag{2}$$

Then $A_{\max} = A(u_{\min})$ is the event's peak amplification, which should be the same in all passbands. For observations of an event in j passbands (perhaps from multiple sites), there are then $N = 3 + j$ free-fit parameters in an overall joint fit. The fits were performed by χ^2 minimization using the function minimization program MINUIT (James 1994). Table 1 shows the parameters and error estimates obtained for the Mount Stromlo and CTIO data both as independent fits and with all three passbands combined.

TABLE 1

FIT PARAMETERS AND ERRORS FROM MINUIT FOR THE CTIO AND MOUNT STROMLO DATA SETS ALONE AND COMBINED

	CTIO		MOUNT STROMLO		COMBINED FIT	
PARAMETER	Value	Error	Value	Error	Value	Error
t_0 (days) ...	599.782	0.018	599.832	0.026	599.775	0.014
$\hat{t}$ (days)	18.907	0.165	19.994	0.241	19.202	0.128
$A_{\max}$	3.466	0.013	3.565	0.025	3.487	0.011
f_{0R}	0.5374	0.0017	...	...	0.5339	0.0015
f_{0r}	...	...	0.7878	0.0043	0.8016	0.0030
f_{0b}	...	...	0.7989	0.0056	0.8143	0.0044
χ^2	1.01	...	1.04	...	1.10	...

NOTE.—Time of maximum amplification, t_0, is expressed as JD − 2,449,000. The errors are formal 1 σ values obtained from $\Delta\chi^2 = 1$.

Not surprisingly, the superior seeing at CTIO produces photometry with significantly smaller uncertainties. Figure 1 displays the three time series with the best-fit light curve superimposed. Figure 2 shows the residuals in the CTIO and Mount Stromlo data, after subtracting the microlensing light-curve fit from the data, using the appropriate baseline in each passband. Any light-curve fine structure would be apparent in this plot, and, in particular, the CTIO data would be sensitive to effects at the ~1% level. This is sufficient sensitivity to detect most of the physical processes of interest.

Although in this particular event there is not a detectable signal that departs from the ideal microlensing curve, there have been multiple cases in which the survey data alone have

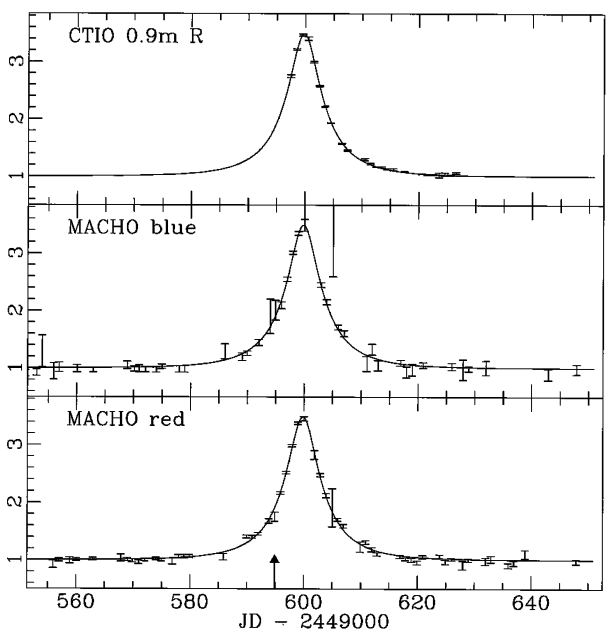

FIG. 1.—Light curves of the event averaged over 1 day bins for each of the three passbands. The vertical axis is in units of flux amplification relative to the fitted baseline. The time of the alert system trigger is indicated by the arrow in the bottom panel. The best-fitting microlensing light curve is superimposed.

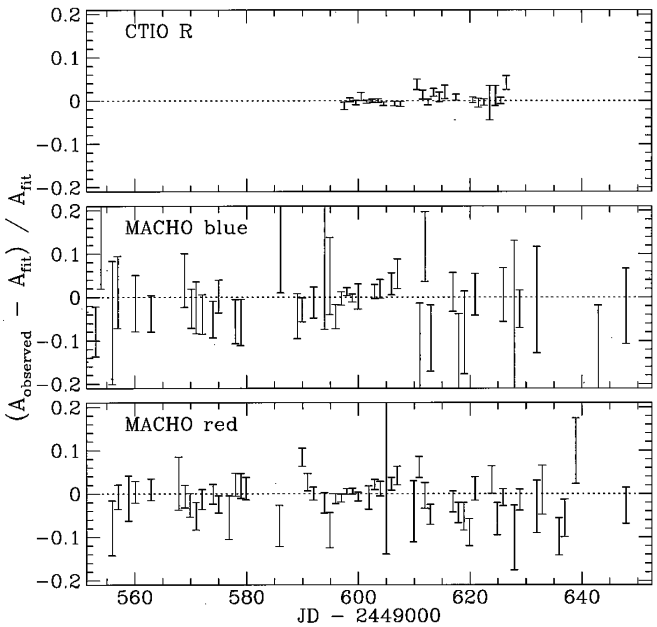

FIG. 2.—The fit residuals averaged over 1 day bins after subtracting the best-fitting light curve expressed as $(A_{observed} - A_{fit})/A_{fit}$.

detected light-curve fine structure (Bennett et al. 1995; Alcock et al. 1995c, 1996b). Rapid, continual, high-accuracy follow-up observations of microlensing events detected in real time should greatly increase the detection of this fine structure.

We are particularly grateful to Doug Reynolds for his skillful implementation of the alert software. We are very grateful for the skilled support given our project by the technical staffs at the Mount Stromlo and CTIO Observatories. We thank the NOAO for making nightly use of the CTIO 0.9 m telescope possible. Work performed at LLNL is supported by the DOE under contract W7405-ENG-48. Work performed by the Center for Particle Astrophysics on the UC campuses is supported in part by the Office of Science and Technology Centers of NSF under cooperative agreement AST-8809616. Work performed at MSSSO is supported by the Bilateral Science and Technology Program of the Australian Department of Industry, Technology and Regional Development. K. G. acknowledges a DOE OJI grant, and C. W. S. and K. G. thank the Sloan Foundation for their support. C. W. S. also thanks the Packard Foundation for their generous support.

REFERENCES

Alard, C., Mao, S., & Guibert, J. 1995, A&A, 300, L17
Alcock, C., et al. 1993, Nature, 365, 621
———. C., et al. 1994, IAU Circ., 6068
———. C., et al. 1995a, Phys. Rev. Lett., 74, 2867
———. C., et al. 1995b, ApJ, 445, 133
———. C., et al. 1995c, ApJ, 454, L125
———. C., et al. 1996a, ApJ, 461, 84
———. C., et al. 1996b, ApJ, submitted
Ansari, R., et al. 1995, preprint astro-ph/9511073
Aubourg, E., et al. 1993, Nature, 365, 623
Benetti, S., Pasquini, L., & West, R. M. 1995, A&A, 294, L37
Bennett, D. P., et al. 1994, in AIP Conf. Proc. 316, Dark Matter, ed. S. Holt & C. Bennett (New York: AIP), 77
Bennett, D. P., et al. 1995, in ASP Conf. Proc. 88, Symposium on Clusters, Lensing, and the Future of the Universe, ed. V. Trimble & A. Reisenegger (San Francisco: ASP), 95
Dwek, E., et al. 1995, ApJ, 445, 716
Gould, A. 1994, ApJ, 421, L71
Gould, A., & Loeb, A. 1992, ApJ, 396, 104
Griest, K. 1991, ApJ, 366, 412
Griest, K., et al. 1991, ApJ, 372, L79
James, F. 1994, MINUIT, Function Minimization and Error Analysis (CERN Program Library Long Writeup D506)
Mao, S., & Paczyński, B. 1991, ApJ, 374, L37
Marshall, S. L., et al. 1994, in IAU Symp. 161, Astronomy From Wide Field Imaging, ed. H. T. MacGillivray et al. (Dordrecht: Kluwer), 67
Paczyński, B. 1986, ApJ, 304, 1
———. 1991, ApJ, 371, L63
Pratt, M. R., et al. 1995, in Astrophysical Applications of Gravitational Lensing, ed. C. S. Kochanek & J. N. Hewitt (Dordrecht: Kluwer), 221
Schecter, P. L., Mateo, M., & Saha, A. 1993, PASP, 105, 1342
Stetson, P. B. 1987, PASP, 99, 191
———. 1992, in IAU Colloq. 136, Stellar Photometry: Current Techniques and Future Developments, ed. C. J. Butler & I. Elliott (Cambridge: Cambridge Univ. Press), 291
Stubbs, C. W., et al. 1993, Proc. SPIE, 1900, 192
Szymanski, M., et al. 1994, Acta Astron., 44, 387
Udalski, A., et al. 1993, Acta Astron., 43, 289
———. 1994a, Acta Astron., 44, 165
———. 1994b, Acta Astron., 44, 227
———. 1994c, ApJ, 436, L103
Weiland, J. L., et al. 1994, ApJ, 425, L81
Witt, H. J., & Mao, S. 1994, ApJ, 430, 505